

## Experimental band structure of the nearly half-metallic $\text{CuCr}_2\text{Se}_4$ : an optical and magneto-optical study

This article has been downloaded from IOPscience. Please scroll down to see the full text article.

2010 New J. Phys. 12 053039

(<http://iopscience.iop.org/1367-2630/12/5/053039>)

View [the table of contents for this issue](#), or go to the [journal homepage](#) for more

Download details:

IP Address: 188.6.196.231

The article was downloaded on 24/03/2012 at 22:36

Please note that [terms and conditions apply](#).

## Experimental band structure of the nearly half-metallic $\text{CuCr}_2\text{Se}_4$ : an optical and magneto-optical study

S Bordács<sup>1,2,5</sup>, I Kézsmárki<sup>1,2,3</sup>, K Ohgushi<sup>3,4</sup> and Y Tokura<sup>2,3</sup>

<sup>1</sup> Department of Physics, Budapest University of Technology and Economics, and Condensed Matter Research Group of the Hungarian Academy of Sciences, 1111 Budapest, Hungary

<sup>2</sup> Multiferroics Project, ERATO, Japan Science and Technology Agency (JST), Japan, c/o Department of Applied Physics, University of Tokyo, Tokyo 113-8656, Japan

<sup>3</sup> Department of Applied Physics, University of Tokyo, Tokyo 113-8656, Japan

<sup>4</sup> Institute for Solid State Physics, University of Tokyo, Kashiwanoha, Kashiwa, Chiba 277-8581, Japan

E-mail: [bordacs.sandor@wigner.bme.hu](mailto:bordacs.sandor@wigner.bme.hu)

*New Journal of Physics* **12** (2010) 053039 (10pp)

Received 4 January 2010

Published 26 May 2010

Online at <http://www.njp.org/>

doi:10.1088/1367-2630/12/5/053039

**Abstract.** Diagonal and off-diagonal optical conductivity spectra have been determined from the measured reflectivity and magneto-optical Kerr effect over a broad range of photon energies in the itinerant ferromagnetic phase of  $\text{CuCr}_2\text{Se}_4$  at various temperatures down to  $T = 10$  K. Besides the low-energy metallic contribution and the lower-lying charge transfer transition at  $E \approx 2$  eV, a sharp and distinct optical transition was observed in the mid-infrared region around  $E = 0.5$  eV with huge magneto-optical activity. This excitation is attributed to a parity allowed transition through the Se–Cr hybridization-induced gap in the majority spin channel. The large off-diagonal conductivity is explained by the high-spin polarization in the vicinity of the Fermi level and the strong spin–orbit interaction for the related charge carriers. The results are discussed in connection with band structure calculations.

<sup>5</sup> Author to whom any correspondence should be addressed.

## Contents

<b>1. Introduction</b>	<b>2</b>
<b>2. Experiment</b>	<b>3</b>
<b>3. Results and discussion</b>	<b>3</b>
<b>4. Conclusions</b>	<b>9</b>
<b>Acknowledgments</b>	<b>9</b>
<b>References</b>	<b>9</b>

## 1. Introduction

The ferrimagnetic metal  $\text{CuCr}_2\text{Se}_4$  shows the highest critical temperature  $T_c = 430$  K among chromium spinel chalcogenides [1]. Although the lattice constants of the ferromagnetic semiconductors  $\text{CdCr}_2\text{S}_4$  and  $\text{CdCr}_2\text{Se}_4$  differ by only 1–4%, their ferromagnetism is considerably weakened by the complete filling of the valence band as reflected by  $T_c = 85$  and 129 K, respectively [1].  $\text{CuCr}_2\text{Se}_4$  exhibits a large magneto-optical Kerr effect (MOKE) in the near-infrared photon energy region at room temperature, which makes this compound a promising candidate for magneto-optical devices [2, 3]. Materials from the same family show interesting magneto-transport phenomena, like the colossal magnetoresistance [4] in  $\text{Fe}_{1-x}\text{Cu}_x\text{Cr}_2\text{S}_4$  and the colossal magnetocapacitance [5] in  $\text{CdCr}_2\text{S}_4$ . Moreover, recent band structure calculations indicate that  $\text{CuCr}_2\text{Se}_4$  is almost half-metallic [6]–[9], and the density of states for spin-down electrons can be fully suppressed with cadmium doping, i.e. a perfect half-metallic situation can be realized [9].

The strong ferrimagnetism in  $\text{CuCr}_2\text{Se}_4$  was first explained by Lotgering and Stapele assuming the mixed-valence state of  $\text{Cr}^{3+}$  and  $\text{Cr}^{4+}$  with the monovalent  $\text{Cu}^+$ ; thus this compound was classified as a d-metal with closed Se 4p shell [10]. In this picture, only the chromium sites are magnetic and the double exchange mechanism between the  $\text{Cr}^{3+}$  and  $\text{Cr}^{4+}$  ions aligns their magnetic moment in parallel. However, early neutron diffraction studies indicated that each chromium is in the  $\text{Cr}^{3+}$  state [11]. Later, Goodenough proposed the copper ions to be divalent  $\text{Cu}^{2+}$  and as a source of magnetism the  $90^\circ$  superexchange to be responsible for the coupling between the  $\text{Cr}^{3+}$  ions through the completely filled Se 4p states [12]. The recent x-ray magnetic circular dichroism (XMCD) measurements of Kimura *et al* [13] settled the long-standing issue of the valence state of  $\text{CuCr}_2\text{Se}_4$ . They have confirmed the  $\text{Cr}^{3+}$  state. However, they have found almost monovalent copper and a delocalized hole in the Se 4p band with a magnetic moment anti-parallel to the moment of the  $\text{Cr}^{3+}$  ions. Based on these experimental results, Saha-Dasgupta *et al* [8] have interpreted the ferrimagnetism in terms of a kinetic-energy-driven mechanism in which hybridization between localized  $\text{Cr}^{3+}$  ions and delocalized Se 4p band results in a hole-mediated exchange. Their density functional calculation indicates the appearance of a hybridization-induced hump-like structure at the Fermi energy only for the up-spin states in accordance with other band structure calculations [7, 9].

In order to have a better understanding of the electronic structure of  $\text{CuCr}_2\text{Se}_4$  and its strong itinerant magnetism, we have investigated the low-energy ( $E = 0.1$ – $4$  eV) charge excitations over the temperature range of  $T = 10$ – $300$  K by determining both diagonal and off-diagonal elements of the optical conductivity tensor. Besides the low-energy response of the metallic carriers and the charge transfer excitations above  $E \gtrsim 2$  eV, we have found a sharp

and distinct optical transition in the mid-infrared region with large magneto-optical activity. We believe that our results are also relevant to the understanding of common transition metal ferromagnets.

## 2. Experiment

Single crystals of  $\text{CuCr}_2\text{Se}_4$  with the typical size  $3 \times 3 \times 0.2 \text{ mm}^3$  were grown by the chemical vapor transport method. Details of the preparation and the structure characterization are given elsewhere [14]. All the optical measurements were carried out with nearly normal incidence on the as-grown (111) surface. In order to determine the diagonal optical conductivity, reflectivity spectra were measured over a broad energy range ( $E = 0.08\text{--}26 \text{ eV}$  and  $E = 0.08\text{--}5 \text{ eV}$  at room and low temperatures, respectively) to facilitate proper Kramers–Kronig transformation. We have measured the complex magneto-optical Kerr angle  $\Phi_{\text{Kerr}} = \theta_{\text{Kerr}} + i\eta_{\text{Kerr}}$ , which allows the direct determination of off-diagonal conductivity, in the range  $E = 0.12\text{--}4 \text{ eV}$ , with a polarization modulation technique [15]. In the mid-infrared region, a Fourier transform infrared spectrometer was combined with a ZnSe photoelastic modulator (Hinds, II/ZS50) [14] to perform measurements down to as low an energy as  $E = 0.12 \text{ eV}$ , whereas above  $E > 0.7 \text{ eV}$  a  $\text{CaF}_2$  photoelastic modulator (Hinds, I/CF50) and a grating spectrometer were used. The external magnetic field  $B = \pm 0.25 \text{ T}$  was applied by a permanent magnet along the [111] easy axis of the magnetization, which was parallel to the propagation direction of the light, as well. In the above arrangement, the conductivity tensor has the following form:

$$\sigma = \begin{bmatrix} \sigma_{xx} & \sigma_{xy} & 0 \\ -\sigma_{xy} & \sigma_{xx} & 0 \\ 0 & 0 & \sigma_{zz} \end{bmatrix}. \quad (1)$$

In our notation, the  $x$ -,  $y$ - and  $z$ -directions do not correspond to the main cubic axes, as  $z$  is chosen parallel to the [111] easy axis.

## 3. Results and discussion

The temperature dependence of the reflectivity and the diagonal optical conductivity spectra are shown in figure 1. We identified the different contributions to the optical conductivity as follows. The first charge transfer peak is centered on  $E = 2.75 \text{ eV}$ , which we assign to the  $\text{Se } 4p \rightarrow \text{Cr } 3d$  transition in agreement with previous optical data on a broad variety of chromium spinel oxides and chalcogenides [14]. This transition was assigned as an intra-atomic  $3d^3 \rightarrow 3d^24p$  and  $3d^3 \rightarrow 3d^24s$  excitation by Brändle *et al* [3], which seems to be unlikely as the position and oscillator strength of this transition show a large variation among the different chromium spinels. Furthermore, the chromium  $4p$  and  $4s$  bands are located at higher energies in these compounds, which also excludes their assignment [14]. It has a low-energy shoulder located at  $E = 1.9 \text{ eV}$ , which likely originates from the on-site chromium  $d\text{--}d$  transition, since this structure is common for chromium spinels insensitive to the change of the other cation [14]. This originally dipole-forbidden transition becomes allowed by hybridization with the ligand, which results in a fairly small oscillatory strength. The spectral structures become distinct as the

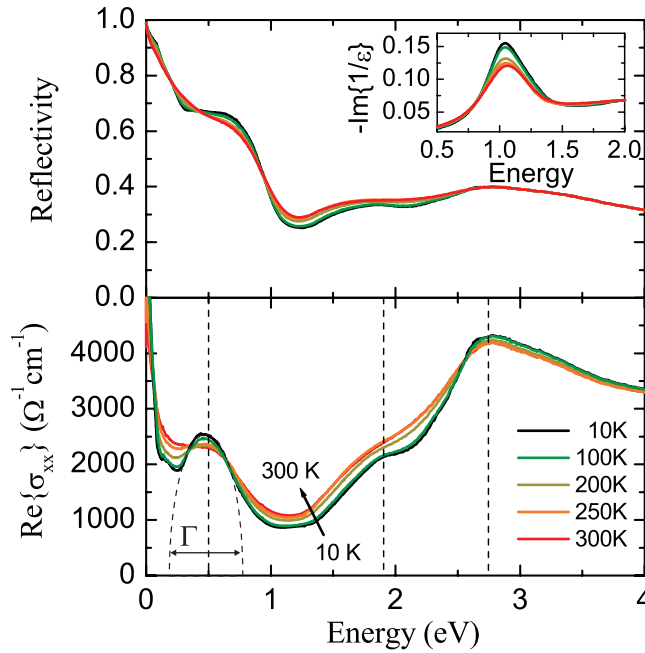


**Figure 1.** Upper and lower panels: the reflectivity and optical conductivity spectra of  $\text{CuCr}_2\text{Se}_4$  at various temperatures. Three main features are indicated by dashed lines. The first charge transfer excitation ( $\text{Se } 4p \rightarrow \text{Cr } 3d$ ) appears at  $E = 2.75 \text{ eV}$  with a low-energy shoulder at  $E = 1.9 \text{ eV}$  due to on-site  $d-d$  transition of the chromium ions. In addition to the low-energy metallic peak, a strong transition is present in the mid-infrared region (at  $E = 0.5 \text{ eV}$ ) with a characteristic width of  $\Gamma \approx 0.5 \text{ eV}$ . In the inset, the maximum of the loss-function indicates the plasma frequency at  $\hbar\omega_{\text{pl}} \approx 1 \text{ eV}$ .

temperature decreases. In the low-energy region ( $E \lesssim 0.1 \text{ eV}$ ), metallic conductivity appears. Although it does not closely follow a Drude-like behavior, a moderate scattering rate—estimated to be  $\gamma \approx 0.03 \text{ eV}$  at  $T = 10 \text{ K}$ —was found. The small residual resistivity determined by dc experiments [14],  $\rho_0 = 10 \mu\Omega \text{ cm}$ , is not typical of bad metals with strongly correlated  $d$  band. Between the low-energy metallic term and the first charge transfer excitation, a distinct peak appears at  $E = 0.5 \text{ eV}$ . In spite of its closeness to the metallic continuum, it becomes sharp and clearly distinguishable at low temperatures characterized by a width of  $\Gamma \approx 0.5 \text{ eV}$ . In the inset of figure 1, the maximum of the loss-function signals a plasma frequency of  $\hbar\omega_{\text{pl}} \approx 1 \text{ eV}$ , which increases by only 4% as the temperature decreases to  $T = 10 \text{ K}$ . This implies only tiny changes in the carrier concentration as a function of temperature.

The magneto-optical Kerr spectra are presented in figure 2 at room temperature and at the lowest temperature  $T = 10 \text{ K}$ . These results are in good agreement with Kerr spectra previously reported at room temperature for  $E > 0.6 \text{ eV}$  [3]. The MOKE signal reaches its maximum around  $E = 1 \text{ eV}$ , where Kerr ellipticity exhibits a peak, while Kerr rotation has a dispersive line shape with the maximal values of  $\eta_{\text{Kerr}} = 1.9^\circ$  and  $\theta_{\text{Kerr}} = -1^\circ$ , respectively. Although magnetization is almost constant below room temperature, the MOKE is enhanced by 45% down to  $T = 10 \text{ K}$ .

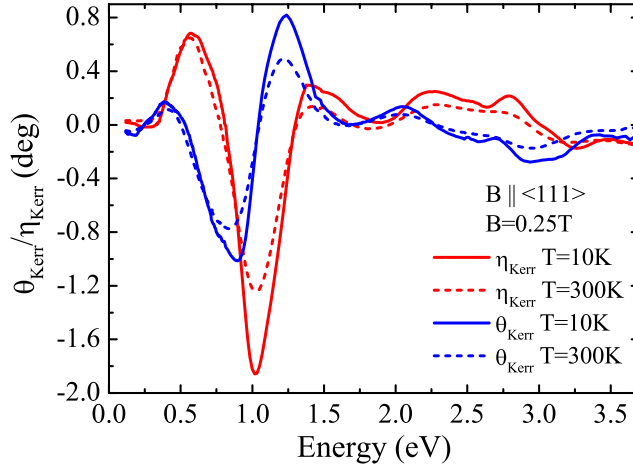


**Figure 2.** The spectra of the magneto-optical Kerr parameters at room temperature and  $T = 10$  K. The Kerr ellipticity shows a peak at  $E = 1$  eV due to the plasma resonance and its maximal value increases to  $\eta_{\text{Kerr}} = 1.9^\circ$  as the temperature decreases to  $T = 10$  K, corresponding to the sharpening of the plasma edge. The Kerr rotation reaches the value  $\theta_{\text{Kerr}} = 1.2^\circ$  in the same region.

From the complex Kerr angle, we have calculated the off-diagonal conductivity according to the following relation:

$$\Phi_{\text{Kerr}} = \theta_{\text{Kerr}} + i\eta_{\text{Kerr}} = -\frac{\sigma_{xy}}{\sigma_{xx}\sqrt{1 + (4\pi i/\omega)\sigma_{xx}}}, \quad (2)$$

where  $\sigma_{xx}$  and  $\sigma_{xy}$  are the elements of the complex optical conductivity tensor. The Kerr rotation and ellipticity describe the phase shift and the intensity difference, respectively, between left and right circularly polarized light upon normal-incidence reflection from a magnetic surface. The corresponding results are presented in figure 3.

In spite of the large MOKE around  $E = 1$  eV, neither off-diagonal nor diagonal conductivity shows any specific optical excitation in this energy region. The large enhancement of the MOKE signal corresponds to the plasma resonance at  $\hbar\omega_{\text{pl}} \approx 1$  eV; it is caused by the strong minimum of the denominator of equation (2) rather than by an increase of off-diagonal conductivity [3, 16]. The almost perfect cancellation of this resonance in off-diagonal conductivity indicates the appropriateness of the Kramers–Kronig transformation for reflectivity. When the optical excitations are broad compared to the magnetically induced splitting of these transitions for the two circular polarizations, the Kerr parameters  $\theta_{\text{Kerr}}$  and  $\eta_{\text{Kerr}}$  are proportional to the derivative of the reflectivity:

$$\eta_{\text{Kerr}} = \frac{1}{2} \frac{r_+^2 - r_-^2}{r_+^2 + r_-^2} \propto \frac{1}{R(E)} \frac{\partial R(E)}{\partial E}, \quad (3)$$

$$\theta_{\text{Kerr}} = \frac{1}{2} (\phi_+ - \phi_-) \propto \frac{\partial \phi(E)}{\partial E},$$

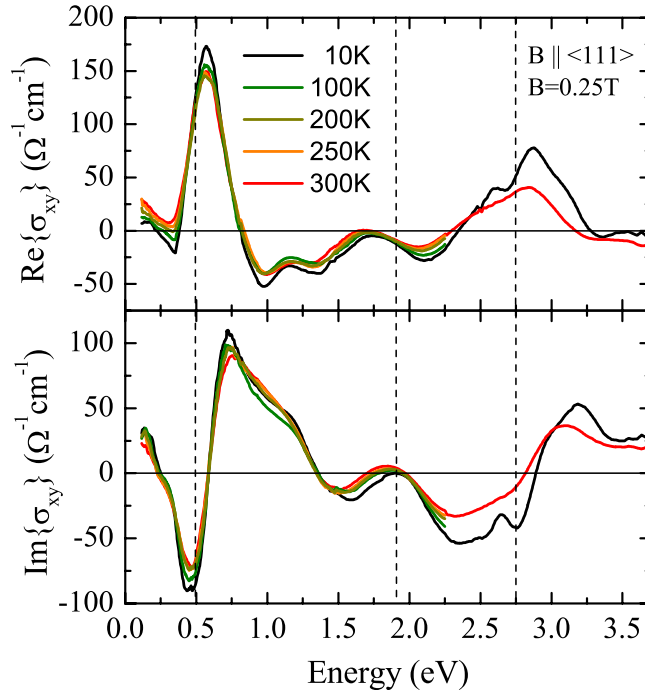


**Figure 3.** The off-diagonal conductivity determined from the magneto-optical Kerr spectra. The plasma edge resonance observed in the Kerr effect is cancelled out, which indicates that the Kramers–Kronig transformation was performed properly. The dashed lines with labels indicate the same transition as in figure 1. The transition at  $E = 0.5$  eV appears large, while the Se 4p→Cr 3d charge transfer excitation also has considerable magneto-optical activity.

where  $\tilde{r}_{\pm} = r_{\pm}e^{i\phi_{\pm}}$  are the Fresnel coefficients for the right and left circularly polarized photons, and  $R(E) = (r_{+}^2 + r_{-}^2)/2$  and  $\phi(E)$  are the reflectivity and the corresponding phase. The sudden decrease in reflectivity near the plasma edge, which generates the large MOKE signal, is sensitive to the slope of the reflectivity, which becomes steeper as the lifetime increases towards low temperatures, causing considerable temperature dependence in the region of plasma resonance.

The real part of the off-diagonal conductivity (shown in figure 3) is dominated by two main structures, namely a broader hump around  $E = 2.75$  eV and a resonance-like peak centered at  $E = 0.5$  eV. The dispersive line shape in the imaginary part of the off-diagonal conductivity and also the corresponding large values— $\text{Im}\{\sigma_{xy}\} = 53 \Omega^{-1} \text{cm}^{-1}$  and  $\text{Im}\{\sigma_{xy}\} = 110 \Omega^{-1} \text{cm}^{-1}$  at  $T = 10$  K, respectively—are suggestive of parity allowed transitions, which is reasonable for the Se 4p→Cr 3d charge transfer transition at  $E = 2.75$  eV. The magnitude of the low-energy part of the off-diagonal conductivity enlarged in figure 4 is very close to that of the dc Hall effect obtained at the same magnetic field [17], except for  $T = 10$  K, where  $\sigma_{\text{Hall}} = 300 \Omega^{-1} \text{cm}^{-1}$ . As the temperature decreases, the low-energy tail of the real part is considerably reduced in contrast to the temperature-independent behavior of the magnetization. This may indicate that a non-perturbative treatment of the spin–orbit coupling is also necessary to describe the low-energy off-diagonal conductivity, as it was formerly proposed for the dc anomalous Hall effect [17, 18].

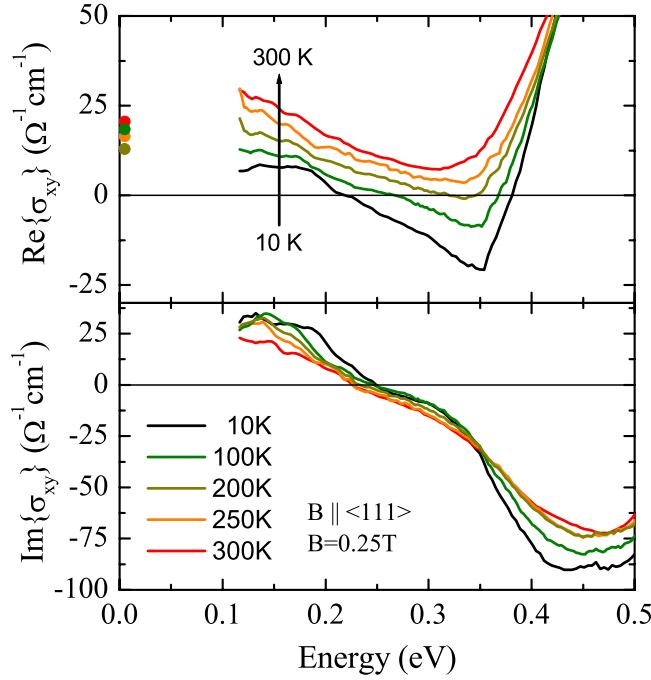


**Figure 4.** The low-energy part of the off-diagonal conductivity. The dc values are reproduced from Hall resistivity measurements performed at the same magnetic field by Lee *et al* [17].

The relations between the elements of the optical conductivity tensor and the underlying microscopic optical processes are described by the Kubo formula:

$$\begin{aligned} \text{Re}\{\sigma_{xx}\} &= \frac{\pi e^2}{2m^2 V \hbar \omega} \sum_{i,f} [1 - f(\varepsilon_f)] f(\varepsilon_i) \{ |\langle f | \Pi_+ | i \rangle|^2 + |\langle f | \Pi_- | i \rangle|^2 \} [\delta(\omega_{fi} - \omega) + \delta(\omega_{fi} + \omega)], \\ \text{Im}\{\sigma_{xy}\} &= \frac{\pi e^2}{4m^2 V \hbar \omega} \sum_{i,f} [1 - f(\varepsilon_f)] f(\varepsilon_i) \{ |\langle f | \Pi_+ | i \rangle|^2 - |\langle f | \Pi_- | i \rangle|^2 \} [\delta(\omega_{fi} - \omega) + \delta(\omega_{fi} + \omega)], \end{aligned} \quad (4)$$

where  $\Pi_{\pm} = \Pi_x \pm i\Pi_y$  are the momentum operators in the circular basis. The real part of the diagonal optical conductivity is proportional to the joint density of states for the occupied and unoccupied states multiplied by the electric dipole matrix elements; therefore, it describes the absorption of light for left and right circularly polarized photons on average. On the other hand, the imaginary part of the off-diagonal conductivity is the difference between the absorption spectra corresponding to the two circular polarizations. Contributions from electric dipole processes to off-diagonal optical conductivity are remarkable in ferromagnetic materials—due to the orbital magnetization induced by the spontaneous spin polarization via the spin–orbit interaction—similar to the anomalous Hall effect in the dc limit.

To understand the origin of the optical excitations, the results of the recent band structure calculations [7–9] are summarized schematically in figure 5. The chromium d band is split by the cubic crystal field into a  $t_{2g}$  and an  $e_g$  band. The selenium 4p and the copper 3d states are fully mixed with each other. Furthermore, hybridization between the selenium 4p and the chromium

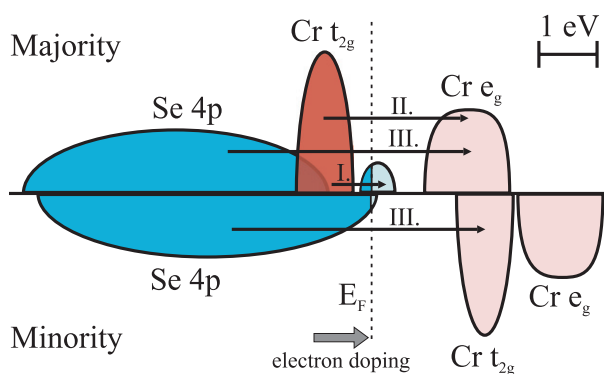


**Figure 5.** The schematic structure of the density of states as determined by density functional calculations [7–9]. The chromium d band is split by the cubic crystal field into a  $t_{2g}$  and an  $e_g$  band. In the majority spin channel, the hybridization between the Se 4p and Cr 3d splits the selenium band and induces a gap just below the Fermi energy. Consequently, one hole appears in the upper branch of the selenium band for majority spins. Complete spin polarization of the charge carriers could be achieved by tiny electron doping [9]; previous band structure calculations indicated that  $x \sim 10\text{--}20\%$  Br, Cd, Zn, etc substitution results in a half metallic state. The thin, black arrows indicate the excitations observed in both the diagonal and the off-diagonal conductivity spectra in the energy region of  $E = 0.1\text{--}4\text{ eV}$ , with the same labels as those used in figures 1 and 3. Processes in the close vicinity of the Fermi level, responsible for the metallic conduction dominating the diagonal optical conductivity for  $E < 0.1\text{ eV}$ , are not labeled in the figure.

$t_{2g}$  induces a gap just below the Fermi energy in the majority spin channel. As a consequence, states from the Se 4p band are shifted above the Fermi level (referred to as ‘hump in the density of states’ in the Introduction); thus holes appear in the majority spin channel. The main optical transitions observed in the experiments are also indicated in the figure.

Our optical and magneto-optical study confirms the results of the band structure calculations both in the close vicinity of the Fermi energy and on the scale of a few eV. In agreement with the theoretical results, we explain the transition at  $E = 0.5\text{ eV}$  as excitations through the hybridization-induced gap. The high oscillator strength is due to the parity difference between the initial and the final states. The large off-diagonal conductivity is possibly due to the strong spin–orbit coupling for the delocalized electrons with a strong selenium character ( $E_{SO} \approx 0.5\text{ eV}$ ) and the highly spin-polarized states in the  $\sim 1\text{ eV}$  vicinity of the Fermi level [7, 9]. The shift of this transition towards higher energy in  $\text{CuCr}_2\text{Se}_{3.7}\text{Br}_{0.3}$  was reported in a previous optical and magneto-optical study [3], which is consistent with the present assignment of the  $E = 0.5\text{ eV}$  peak since bromine substitution increases the Fermi energy by adding electrons to the system.

The first charge transfer excitations around  $E = 2.75\text{ eV}$ , with a remarkable oscillator strength and magneto-optical activity, are attributed to the Se 4p→Cr 3d transition, while the excitation at  $E = 1.9\text{ eV}$  is assigned to on-site d–d transitions of chromium ions. These are in overall agreement with the numerical calculations, although the transition energies are somewhat higher in the experiment [7–9]. The contribution of the d–d transition to the

off-diagonal conductivity is small compared to that of the charge transfer transition. Besides the reduced oscillator strength of the d–d transition due to its dipole-forbidden nature, it is likely caused by the fairly small spin–orbit coupling for chromium ( $E_{SO} = 0.09$  eV) [7].

The measurement of the off-diagonal conductivity helps greatly in extracting the optical transition found around  $E = 0.5$  eV, since its large magneto-optical activity dominates over the contribution from the metallic charge carriers (damped cyclotron resonance) contrary to the case of the diagonal conductivity.

#### 4. Conclusions

We have measured the reflectivity and MOKE over a broad energy range ( $E = 0.08$ – $26$  eV and  $E = 0.1$ – $4$  eV, respectively) at various temperatures down to  $T = 10$  K and evaluated the elements of the optical conductivity tensor. Our room temperature spectra are in accord with the previous reflectivity and MOKE data of Brändle *et al* [2, 3]. However, the extension of the experiment to the mid-infrared region allows us to investigate the charge dynamics close to the Fermi energy. Furthermore, the low temperature measurements help us to separate different excitations in the optical conductivity due to the increased lifetime. The diagonal and off-diagonal optical conductivity spectra determined from the experiments are consistent with the results of previous band structure calculations [7–9] over the whole energy region. Based on this band structure schema, supported by our results, we expect that the perfect half-metallic situation can be realized by tiny electron doping, i.e. by  $x \sim 10$ – $20\%$  Br, Cd, Zn, etc substitution, as predicted by Butler *et al* [9]. At low energies a metallic peak is present, while the  $E \gtrsim 2$  eV region is dominated by the first charge transfer transition Se 4p→Cr 3d. Moreover, we have observed a distinct optical transition around  $E = 0.5$  eV, which we attribute to excitations through the Se–Cr hybridization-induced gap. This transition has a huge magneto-optical activity due to the high-spin polarization in the  $\sim 1$  eV vicinity of the Fermi level and its parity-allowed nature. The corresponding sharp feature in the off-diagonal conductivity dominates over the contribution from the metallic electrons. On this basis, we found that the hybridization between the Cr  $t_{2g}$  and Se 4p bands plays a crucial role in the strong itinerant ferromagnetism of  $\text{CuCr}_2\text{Se}_4$ . A large enhancement of the Kerr effect was also observed around the plasma edge.

#### Acknowledgments

This work was supported by a Grant-In-Aid for Scientific Research from MEXT of Japan and by the Hungarian Research Funds OTKA PD75615, NK72916 and Bolyai 00256/08/11.

#### References

- [1] Hellege K-H (ed) 1980 *Magnetic and Other Properties of Oxides and Related Compounds* vol III, part 12b (Berlin: Springer)
- [2] Brändle H, Schoenes J, Wachter P, Hulliger F and Reim W 1990 *Appl. Phys. Lett.* **56** 2602
- [3] Brändle H, Schoenes J, Wachter P, Hulliger F and Reim W 1991 *J. Magn. Magn. Mater.* **93** 207
- [4] Ramirez A P, Cava R J and Krajewski J 1997 *Nature* **386** 156
- [5] Hemberger J, Lunkenheimer P, Fichtl R, Krug von Nidda H A, Tsurkan V and Loidl A 2005 *Nature* **434** 364
- [6] Ogata F, Hamajima T, Kambara T and Gondaira K I 1982 *J. Phys. C: Solid State Phys.* **15** 3483

- [7] Antonov V N, Antropov V P, Harmon B N, Yaresko A N and Perlov A Ya 1999 *Phys. Rev. B* **59** 14552
- [8] Saha-Dasgupta T, De Raychaudhury M and Sarma D D 2007 *Phys. Rev. B* **76** 054441
- [9] Wang Y H A, Gupta A, Chshiev M and Butler W H 2008 *Appl. Phys. Lett.* **92** 062507
- [10] Lotgering F K and Stapele R P 1967 *Solid State Commun.* **5** 143
- [11] Colominas C 1966 *Phys. Rev.* **153** 558
- [12] Goodenough J B 1969 *J. Phys. Chem. Solids* **30** 261
- [13] Kimura A, Matsuno J, Okabayashi J, Fujimori A, Shishidou T, Kulatov E and Kanomata T 2001 *Phys. Rev. B* **63** 224420
- [14] Ohgushi K, Okimoto Y, Ogasawara T, Miyasaka S and Tokura Y 2008 *J. Phys. Soc. Japan* **77** 034713
- [15] Sato K 1981 *Japan. J. Appl. Phys.* **20** 2403
- [16] Feil H and Haas C 1987 *Phys. Rev. Lett.* **58** 65
- [17] Lee W-L, Watauchi S, Miller V L, Cava R J and Ong N P 2004 *Science* **303** 1647
- [18] Yao Y, Liang Y, Xiao D, Niu Q, Shen S-Q, Dai X and Fang Z 2007 *Phys. Rev. B* **75** 020401